Program Digest, 2019 IEEE International Ultrasonics Symposium (IUS)
Glasgow, Scotland, October 6-9, 2019

Ultrasound Dereverberation/Deconvolution Filtering Based on Gaussian Mixture Modeling

Abhishek Sahoo
Electrical and Computer Engineering
University of Minnesota, Twin Cities
Minneapolis, USA
sahoo015@umn.edu

Anas Al-Hussayen
Electrical and Computer Engineering
University of Minnesota, Twin Cities
Minneapolis, USA
alhus010@umn.edu

Nayef Alshamlan
Electrical and Computer Engineering
University of Minnesota, Twin Cities
Minneapolis, USA
alsha027@umn.edu

Emad S Ebbini
Electrical and Computer Engineering
University of Minnesota, Twin Cities
Minneapolis, USA
emad@umn.edu

***Abstract*—Reverberation is a significant source of degradation in ultrasound imaging in regions with mixtures of scattering structures. Its effects vary from subtle to pronounced, but they can degrade both spatial and contrast resolutions. Deconvolution filters based on the system impulse response often improve axial resolution in uniform speckle regions, but may not perform optimally in complex scattering regions. We have developed an algorithm for the design of a dereverberation/deconvolution filter (DDF) based on a Gaussian mixture model (GMM) of echo data from heterogeneous tissues. RF data were collected using the LA 14-5 probe on a SonixRP scanner while imaging the femoral artery of a familial hypercholesterolemic swine in vivo under approved protocol. The tissues surrounding the target vessel included muscle, fat and connective tissue. Correlation cell sizes and echo statistics differed substantially, which justified the use of the GMM of order 5 for this FOV. The DDF filter was derived from A-lines passing through the vessel to capture short- and long-range spatial correlations, a key feature for estimating the GMM parameters. An expectation-maximization algorithm was used to derive the DDF coefficients while updating the GMM. The algorithm converges within a few iterations to a causally stable IIR filter with well-behaved impulse response. Further iterations allow the DDF to equalize the frequency response and achieve deconvolution without the need for regularization.**

***Index Terms*—pseudo-inverse operator, expectation maximization, ultrasound clutter.**

I. Introduction

Revereberation is a major source of clutter in ultrasound imaging, which results in visible degradation and loss of contrast in low scattering regions [1]. In some cases reverberation is visible and can be easily interpreted, e.g. healthy vessel walls produce distinct reverberation patterns in some cases. On the other hand, it can also be more subtle, leading to distortion of local speckle statistics and, consequently, degrading quantitative imaging and other signal processing operations. One area where this form of clutter may be especially significant is speckle tracking for elastography and themography [2]. In these applications, significant reverberation components appearing at a given echo location may produce speckle shift artifacts, which results in reduced specificity.

Funded in part by Grant NS 098781 from the National Institute of Health.

Dereverberation has received significant interest in speech and audio signal processing. However, the applicability of the solutions in these areas to medical ultrasound is not straightforward due to the speckle phenomenon. Statistical solutions to the dereverberation problem in ultrasound have been lacking.

We have previously proposed a dereverberation filter in the context of vascular imaging [3] and, separately, a least squares 2D deconvolution filter [4]. In this paper, we proposed a modified version of our dereverberation filter to achieve deconvolution in order to restore or improve axial resolution. We present experimental demonstration of the ability of the DDF filter to simultaneously reduce the reverberation component and improve axial resolution while maintaining contrast and lateral resolution.

II. Materials and Methods

A. Data Acquisition

A Sonix RP (Ultrasonix, Canada) ultrasound scanner loaded with custom designed program is used for M2D pulse-echo data collection. Collected data is then streamlined to a controller PC through Gigabit Ethernet for real-time data processing. The data processing computer can easily handle the intensive computations required by high resolution (both spatial and temporal) speckle tracking and separable 2D post filtering by utilizing a many core GPU (nVIDIA, Santa Clara, CA). A linear array probe (LA14-5/38) was used to acquire all data shown in this paper. The center frequency of the transmit pulse on the probe was 7.5 MHz.

B. In Vivo Image

A cross sectional view of the femoral artery of a swine was imaged using the Sonix RP as part of an approved protocol. The image (Fig. 1) contains several interesting features and exhibits reverberations due to the vessel wall and layered

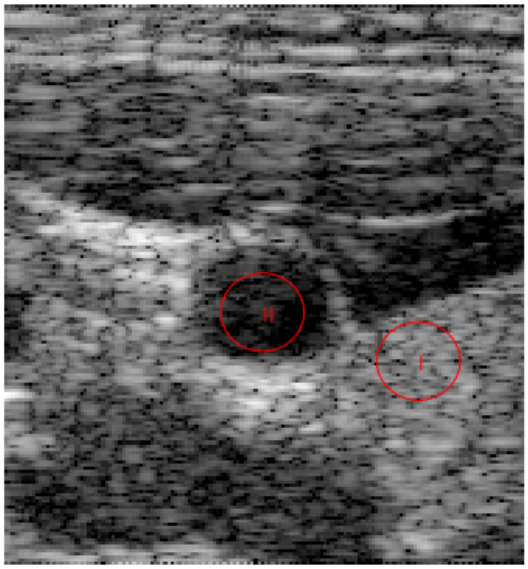

Fig. 1. The original image of the target femoral artery in a swine *in vivo* with two regions identified for quality assessment.

muscle structures. It also contains uniform speckle regions that allowed for measuring the speckle cell size and contrast ratio. The image also contains several sharp boundaries along its axial direction suitable for visual assessment of axial resolution.

C. Receive Signal Models

Linear post-beamforming models were assumed for both filtering schemes described in this paper.However, the dereverberation/deconvolution filter was derived from a more general receive signal model accounting for coherent and incoherent echo components with the coherent component given by:

$$x_c(t,l) = R_{tw} p\left(t - \frac{2z_0}{c}\right) + \sum_{k=1}^{\infty} \alpha_k p\left(t - \frac{2z_0}{c} - \frac{2kd_w}{c}\right) \tag{1}$$

where $p(t) = a(t)e^{j(\omega_0 t + \theta(t))}$ is the analytic transmitted ultrasound pulse, R_{tw} is the reflection coefficient, and d_w is the vessel wall thickness. In (1), R_{tw} represents the tissue-wall reflection coefficient and α_k is a function of the wall-tissue reflection and transmission coefficients [2]. The reflection coefficients are typically small (e.g. $< 10\%$) and the series in (1) is practically 2 to 4 terms for each layer. Unfortunately, the reverberation terms interfere with the echo components from the blood in the vessel. Despite their rapid decay, their amplitude remains high enough to mask the echoes from the blood in a region that extends several millimeters inside the vessel. A dereverberation filter is necessary to unmask the echoes from the blood and allow the 2DST to estimate vector velocity inside the vessel [1].

D. Dereverberation/Deconvolution Filter (DDF)

It is easy to show that the correlation function of the coherent echo component exhibits secondary peaks at $\tau_k = 2kd_w/c$. The amplitude of these peaks diminishes exponentially with k (due to multiple reflection within the wall). These secondary peaks can be estimated from the autocorrelation function of the echo data after baseband conversion. Results from actual vascular imaging experiments suggest that a Gaussian mixture model (GMM) may be most appropriate for modeling the probability density function (pdf) of the clean echo data. The GMM is also motivated by a number of hypotheses on the scattering by blood (e.g. due to flow or red blood cell aggregation) [5]. We also assume an IIR model for the dereverberation inverse filter

$$y[n] = x[n] - \sum_{k=1}^{N} a_k y[n-k]. \tag{2}$$

The coefficients, $\{a_k\}_{k=1}^{N}$ can be obtained by maximizing the log-likelihood with respect to the GMMs in the flow channel (see [1] for more detail). This leads to a simple update equation for the IIR filter coefficients:

$$a_k[m+1] = a_k[m] + \delta \frac{\partial \mathcal{L}}{\partial a_k[m]} \tag{3}$$

where m is the iteration index and δ is chosen sufficiently small to allow for fine convergence (at the expense of convergence speed). The log-likelihood function, $\mathcal{L}$, is given in [1] and it accounts for the fact that the observed (post-beamformed) samples result from an underlying Gaussian mixture of N_g distributions with $\mathcal{N}(\mu_i, \sigma_i), i = 1, 2, \ldots, N_g$.

As with many data-dependent filtering approaches, the model order selection is an important consideration in filter design. In practice, the model order varies depending on the nature of reverberation, which could vary in both space and time, e.g. the case of pulsating vessels. However, the order can be easily determined if reference, reverberation-free, echo data is available. Fortunately, typical images of vascular anatomies of interest provide multiple opportunities for identifying reference data.

E. Two-dimensional Deconvolution Filter

A two dimensional pseudoinverse operator (2D PIO) filtering algorithm was introduced in [4]. It is based on system model on a Cartesian grid suitable for linear array imaging format. In [3], the 2D PIO was applied to *in vivo* beamformed echo data from a human carotid imaging using the Ultrasonix RP system with L14-5/38 linear array probe. A simulated model for forward propagation was constructed based on the L14-5/38 linear array probe profile with the speed of sound set to be 1540 m/s as in soft tissue. This 2D point spread function (psf) was used to design a 2D deconvolution filter, the 2D PIO, based on the pseudoinverse of a 2-way propagation operator describing the full 2D linear array imaging on a rectilinear grid defined by the number of A-lines and number of RF samples per A-line in an imaging frame. We have shown that, while direct numerical computation of the 2D pseuoinverse operator

is infeasible, an analytical formulation allowed for a simple solution in the Fourier domain, or k-space, given by:

$$s_{K(k,n)} = d^{\dagger}_{k,n} \cdot f_{K(k,n)} \tag{4}$$

where s_K and f_K are the k-space representations of the reconstructed (deconvolved) and beamformed 2D rf data, respectively. The operator $d^{\dagger}_{k,n}$, is the pseuoinverse of the k-space representation of the RF psf given by

$$d^{\dagger}_{k,n} = \frac{d^{*}_{n,k}}{{d_{n,k}}^2 + \beta} \tag{5}$$

where β is a regularization parameter and $d_{k,n}$ is the k-space representation (2D DFT coefficient) of the 2D system impulse response. And the 2D impulse response can be obtained by a simulated model for forward propagation [4].

F. Image Quality Assessment

With reference to Fig. 1, two regions were identified for image quality assessment. Region I, indicated by a circle with `I` inside, was chosen as a uniform speckle region approximately at the same depth of the vessel. Region II, indicated by the circle with `II` inside, was contained within the lumen of the femoral artery. The contrast ratio (CR) was computed as follows:

$$CR = 10 \log_{10} \left[\frac{\overline{I}_I}{\overline{I}_{II}} \right] \tag{6}$$

where $\overline{I}_I$ and $\overline{I}_{II}$ are the mean intensity values for the region I and II respectively. In addition to the contrast measurement, we computed the speckle statistics in a rectangular region containing Region I. Both SNR and speckle cell size were measured as we described in [6].

III. Results and Discussion

The RF data corresponding to image shown in Fig. 1 was processed to derive the DDF filter coefficients after estimating the order of the GMM and the filter. The training data included echoes from A-lines traversing the vessel wall and the proximal muscle layers. Echoes from the uniform speckle region, Region I, was used as reverberation-free data. A GMM order of 5 was used and the the DDF filter of order 15 was derived. In principle, a spatially varying filter may be used in different regions of the image to account for the local statistics. However, this would result in potentially distorted image intensity. We have used the same DDF filter to process all imaging A-lines in order to be able to assess the quality of the resulting image.

It is instructive to examine the frequency response of the derived DDF filter compared to representative echo spectrum (vessel wall region). This is shown in Fig. 2 with the echo power spectrum density shown in blue and the DDF frequency response shown in red. This result clearly illustrates the dual function of the DDF as a dereverberation and a deconvolution filter. The dereverberation function is indicated by ripple throughout the frequency range. This is consistent with the classic spectrum of reverberated signals. The deconvolution function is indicated by the reduction in gain within the center

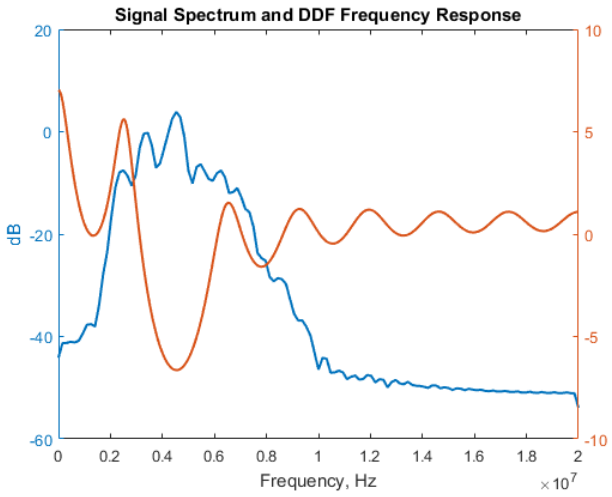

Fig. 2. The PSD of echo data (blue) and the frequency response of the DDF filter.

band of the echo spectrum and the slight gain at the lower frequencies.

The 2DPIO was derived based on the focus settings of the Sonix RP (single transmit focus at 25 mm) and information received from the vendor on the probe geometry. We have also simulated its 2D psf based on the measured impulse response. The formulation of the 2D PIO is least squares one and does not take into account the statistics of the data. The regularization parameter β in (5) was chosen to achieve approximately the same CR ratio as the DDF. In this case, we chose $\beta = 5$. This was a relatively high value, which limited the usefulness of the 2D PIO as a deconvolution filter. In fact, as discussed below, the presence of reverberation is a source of degradation for model-based least square filter formulations, which require heavy regularization.

Fig. 3 shows 50-dB images of the target vessel and surrounding tissues. The leftmost is the original, the middle was obtained by applying a regularized 2D pseudoinverse filter (2D PIO), while the rightmost image was obtained by applying the DDF.

Compared to the original image, the DDF filtered image demonstrate improved axial resolution as measured by the speckle cell size 210 μm vs 340 μm. The lateral speckle cell size was approximately the same for the original and the DDF-processed image at 1.28 mm.

The improvement in axial resolution can be visually appreciated by examining the specular reflection in mid-axial range on the right. The reflector appears to be visually sharper compared with its counterpart in the original image. Furthermore, the speckle region around Region I in Fig. 1 appears to be visually finer, consistent with the speckle cell size measurement. In fact, it is possible that the reduction in CR ratio, i.e. due to reduction in reverberation component in the speckle region being larger than the reduction within the lumen (in Region II).

It is interesting to note that the DDF filtered image shows

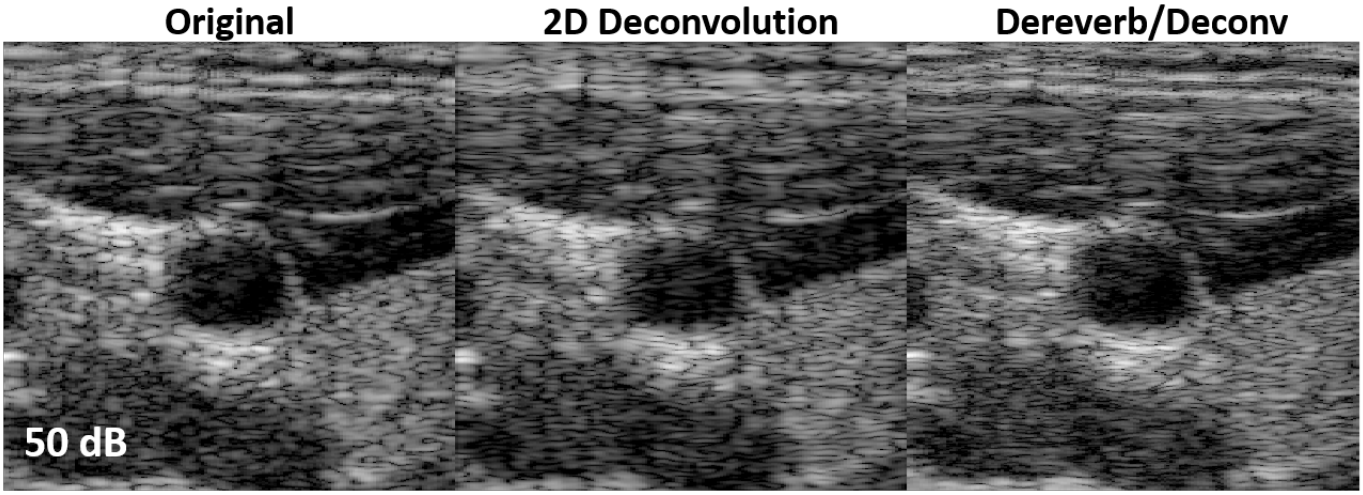

Fig. 3. Images (50 dB) of the original (left), 2D PIO filtered and DDF filtered beamformed echo data.

improved axial resolution throughout the image. This is based on visual comparison of specular reflections in the muscle tissue on top of and the speckle signal in other regions. Therefore, overall, the DDF has improved the resolution as a deconvolution filter while maintaining the contrast.

The 2D PIO also resulted in an improved axial resolution as measured by the speckle cell size. However, the 2DPIO produced artifacts near specular reflections, exhibited by "double" echoes of the specular reflectors throughout the image. This is possibly due to imperfect measurement of the transducer impulse response used for evaluating the 2D PIO coefficients. In fact, this can also be seen by careful examination of the echoes the uniform speckle region around Region I. Therefore, the finer resolution in this case is of questionable value. The lateral resolution was degraded compared to the original. We measured a lateral speckle cell size of 1.79 mm for the 2D PIO processed image compared to 1.28 mm for the original.

We have measured the SNR values around Region I and it was 2.0, 1.78 and 1.92 for the original, 2D PIO filtered and the DDF filtered images, respectively. The result further suggests that the DDF successfully removed some of the clutter that degraded the underlying statistics while improving the axial resolution as a deconvolution filter.

It should be noted that our goal is not to show the inferiority of the 2D PIO to the DDF method. A more careful measurement of the system impulse response might have improved the 2D PIO results. Also, the implementation can be modified to improve the robustness of the method, but these are outside the scope of this paper. We do emphasize, however, that data-dependent filters based on the echo statistics are likely to have that robustness built in.

IV. Conclusions

We have presented *in vivo* imaging results demonstrating the effectiveness of a statistical filtering approach to simultaneously dereverberating and deconvolving ultrasound echo data. The results demonstrate the dereverberation/deconvolution filtering based on GMM statistical modeling produced images with improved axial resolution both quantitatively and perceptually. At the same time, the filtering approach maintained the contrast resolution and lateral resolution. Compared to least squares 2D PIO approach, the DDF appears to be very robust and effective in removing clutter due to reverberation without significant degradation of imaging performance in terms of spatial and contrast resolution.

References

[1] E. S. Ebbini, Y. Wan and D. Liu, "Dereverberation of ultrasound echo data in vascular imaging applications," *2011 IEEE International Conference on Acoustics, Speech and Signal Processing (ICASSP)*, Prague, 2011, pp. 741-744. doi: 10.1109/ICASSP.2011.5946510.

[2] E. S. Ebbini, C. Simon and D. Liu, "Real-Time Ultrasound Thermography and Thermometry [Life Sciences]," in *IEEE Signal Processing Magazine*, vol. 35, no. 2, pp. 166-174, March 2018. doi: 10.1109/MSP.2017.2773338

[3] Y. Wan and E. S. Ebbini, "A 2D post-beamforming filter for contrast restoration in medical ultrasound: in vivo results," *2009 Annual International Conference of the IEEE Engineering in Medicine and Biology Society*, Minneapolis, MN, 2009, pp. 1945-1948. doi: 10.1109/IEMBS.2009.5333460

[4] Y. Wan and E. S. Ebbini, "A post-beamforming 2-D pseudoinverse filter for coarsely sampled ultrasound arrays," in *IEEE Transactions on Ultrasonics, Ferroelectrics, and Frequency Control*, vol. 56, no. 9, pp. 1888-1902, September 2009. doi: 10.1109/TUFFC.2009.1265

[5] K.K. Shung, R.A. Sigelmann, and J.M. Reid, Scattering of ultrasound by blood, *Biomedical Engineering, IEEE Transactions on*, vol. BME-23, no. 6, pp. 460 467, nov. 1976.

[6] R. F. Wagner, M. F. Insana, S. W. Smith, "Fundamental correlation lengths of coherent speckle in medical ultrasonic images", *IEEE Trans. Ultrason. Ferroelectr. Freq. Control*, vol. 35, no. 1, pp. 34-44, Jan. 1988.